



SCIREA Journal of Information Science
and Systems Science

ISSN: 2995-3936

<http://www.scirea.org/journal/ISSS>

January 16, 2024

Volume 8, Issue 1, February 2024

<https://doi.org/10.54647/iss120324>

Design and Implementation of Virtual Maintenance Training System for Heavy Duty Gearbox

Zi-cheng Zhu^{1,*}, Yan Diao¹, Xiang-hui Li¹

¹ China Heavy Truck Group Co.,Ltd,Jinan,Shandong,250116,China

* Corresponding author: zzc_jinan@126.com (Zi-cheng Zhu)

Abstract

By analyzing the structural performance characteristics of a heavy-duty gearbox, based on the modular design thinking and the requirements of the actual maintenance training application, the virtual prototype of a heavy-duty gearbox, such as the construction of three-dimensional model, collision detection, 3d observation, disassembly sequence planning and evaluation of training in the virtual maintenance training simulation platform and maintenance simulation implementation process. A desktop virtual maintenance training system based on EON simulation platform is constructed. The training results show that the system can accurately guide the trainees to complete the gearbox maintenance training tasks correctly, with good operability and interaction.

Keywords: heavy duty gearbox; virtual maintenance; model construction; collision detection; fuzzy evaluation.

1. Preface

The gearbox of a heavy vehicle has the advantages of high transmission efficiency and good stability, and is widely used in tractors, dump trucks, trucks and other heavy trucks, and is loved by users. However, this type of gearbox has high manufacturing cost, complex structure and difficult technical support, which puts forward higher requirements for maintenance personnel. Traditional engineering equipment maintenance is usually combined with the actual machinery on the basis of the use of physical disassembly, video, wall charts, three-dimensional animation and other common auxiliary means ¹. Due to the limitation of environment, cost and condition, it is difficult to achieve ideal training effect. To solve this problem, this paper, with the help of VR technology, combined with the key technology of virtual maintenance training, developed a virtual maintenance training system for gearbox based on EON Studio platform, simulated the maintenance process of gearbox, and provided an accurate and intuitive simulation environment for trainees.

2. Composition of system framework

In full study and analysis of the actual situation of daily maintenance training combined with the needs of trainees, the virtual maintenance training system designed basic training, disassembly training, maintenance training and maintenance training virtual simulation modules. Each training module is connected with each other and does not interfere with each other. It can be carried out continuously or completed independently. The modular system construction of training subjects is shown in Figure 1.

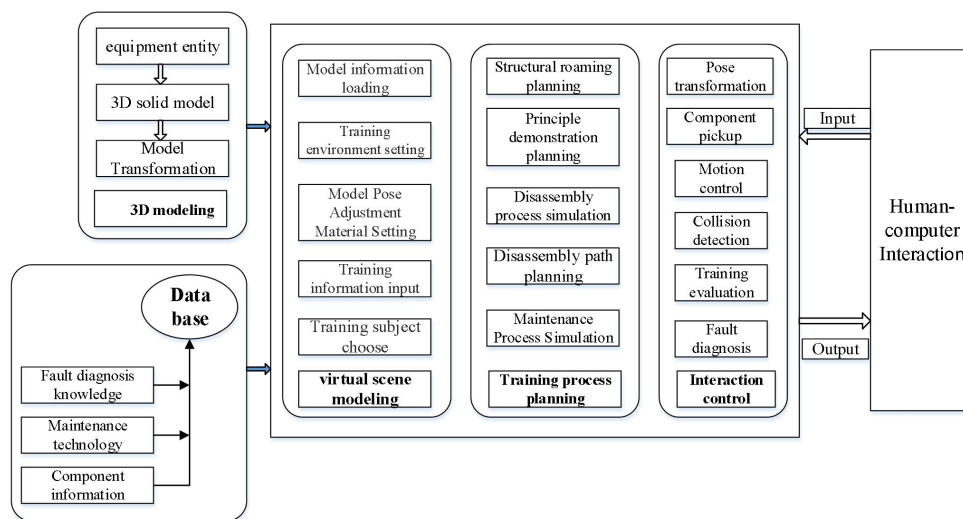


Fig. 1 Construction of modular system of training subjects

3. Key Technology of System

3.1 Construction of 3D Model

The construction of 3D model is the key and foundation of virtual maintenance training system, and the quality of 3D model directly affects the training effect. The complex results of gearbox require comprehensive modeling method to complete the construction of simulation model. NURMS surface modeling method can be adopted for gearbox curved parts. The equation of NURBS surface can be expressed in many ways. A NURBS surface of degree $K \times 2$ can be expressed as follows eq. 1²:

$$P(u, v) = \frac{\sum_{i=0}^m \sum_{j=0}^n w_{i,j} d_{i,j} N_{i,k}(u) N_{j,l}(v)}{\sum_{i=0}^m \sum_{j=0}^n w_{i,j} N_{i,k}(u) N_{j,l}(v)} \quad (1)$$

Wherein, $d_{i,j}$ ($i=0,1,\dots,m$; $j=0,1,\dots,n$) is the control point, which forms a topological rectangular array and forms a control grid, $w_{i,j}$ is the weight factor associated with the control point, $d_{i,j}$; $N_{i,k}(u)N_{j,l}(v)$ are the normal b-spline bases of the parameters u to the k degree and v to the L degree, respectively. They are determined by u nodal vector $U = [u_0, u_1, \dots, u_{m-k+1}]$ and V nodal vector $V = [v_0, v_1, \dots, v_{n-l+1}]$ respectively.

NURBS is ideal for creating smooth, complex models with realistic details. For the modeling of the complex parts of the gearbox, the NURBS fitting surface method combined with splicing and re-modification is adopted. The basic process is shown in Figure 2, and the gearbox constructed by this method is shown in Figure 3.

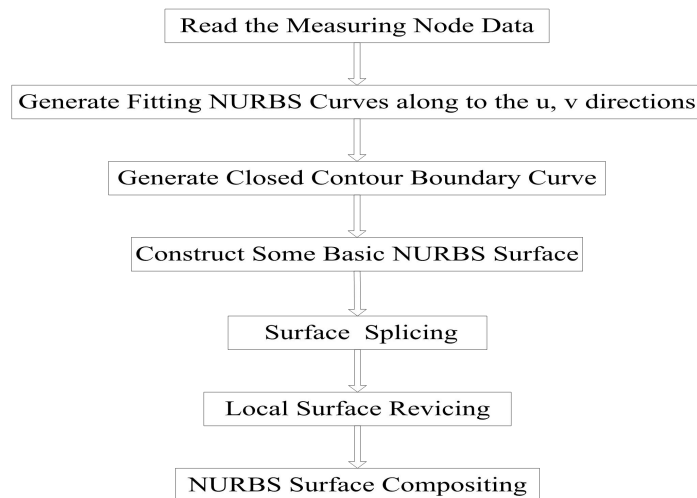


Fig. 2 Flowchart of NURBS surface reconstruction

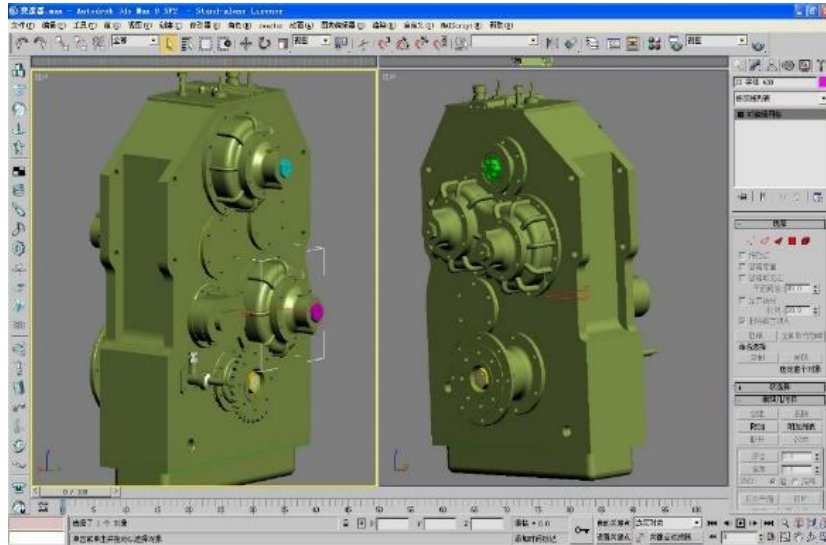


Fig. 3 Construction of gearbox model

3.2 3D Observation Technique in Virtual Environment

Virtual maintenance training environment required to provide relevant training objects, scene and tools such as the real description, in order to ensure the precise location of objects in the virtual environment of maintenance, the system in the process of constructing a virtual environment, and for each object in the virtual scene the absolute coordinates of a fixed (world coordinates) and the relative motion of object coordinates (local coordinates)^{3,4}. When the object moves, the position of the local coordinate system changes correspondingly in the world coordinate system. However, although the graphic elements described, such as points, lines and planes, move with the coordinate system, their directions and poses remain unchanged. The coordinate transformation process can be described by the following homogeneous coordinate matrix:

$$T = \begin{bmatrix} A_{3 \times 3} & B_{3 \times 1} \\ A_{1 \times 3} & B_{1 \times 1} \end{bmatrix} \quad (2)$$

Wherein, matrix $A_{3 \times 3}$ corresponds to geometric transformation, $A_{1 \times 3}$ corresponds to translation transformation, $B_{3 \times 1}$ refers to projection transformation, and $B_{1 \times 1}$ refers to overall proportional transformation.

Objects move in the scene according to the definition of the world coordinate system. However, for the operator, the object is expected to move relative to him, which needs to transform the observation coordinate system to make the observation coordinate system coincide with the world coordinate system. The specific process is as follows: Set the origin

of the world coordinate as (x_0, y_0, z_0) , then observe the translation matrix T from the reference system to the world coordinate system as:

$$T = \begin{bmatrix} 1 & 0 & 0 & -x_0 \\ 0 & 1 & 0 & -y_0 \\ 0 & 0 & 1 & -z_0 \\ 0 & 0 & 0 & 1 \end{bmatrix} \quad (3)$$

The rotation matrix from the observing frame to the world frame depends on the selected positive observing direction. If the observation direction does not coincide with any of the axes, you can use the transformation sequence $R_z \cdot R_y \cdot R_x$ column to overlap the observation and world coordinates. That is, first rotate the Angle γ about the x_w axis of the world coordinate system so that y_v is in the $x_w y_w$ plane. Then rotate the Angle θ about the z_w axis of the world coordinate system to reunite the y_w and y_v axes. Finally, rotate the Angle β about the y_w axis to align the z_w and z_v axes. The rotation sequence matrix is expressed as:

$$R = \begin{bmatrix} \cos \theta \cdot \cos \beta & \sin \theta \cdot \cos \gamma + \cos \theta \cdot \sin \beta \cdot \sin \gamma & \sin \theta \cdot \sin \gamma - \cos \theta \cdot \sin \beta \cdot \cos \gamma \\ -\sin \theta \cdot \cos \beta & \cos \theta \cdot \cos \gamma - \sin \theta \cdot \sin \beta \cdot \sin \gamma & \cos \theta \cdot \sin \gamma + \sin \theta \cdot \sin \beta \cdot \cos \gamma \\ \sin \beta & -\cos \beta \cdot \sin \gamma & \cos \beta \cdot \cos \gamma \end{bmatrix} \quad (4)$$

The rotation interaction of the model in the scenario is shown in Figure 4.

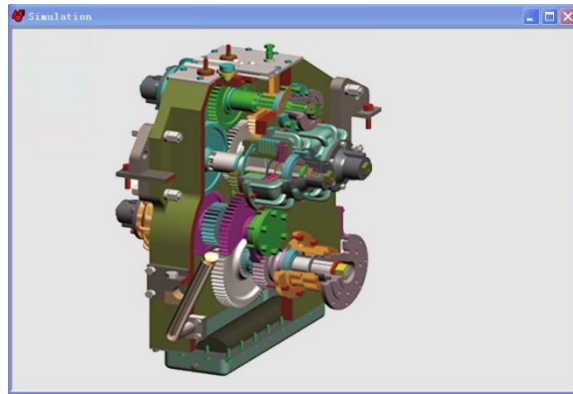


Fig. 4 The rotational interaction of the gearbox in the virtual scene

3.3 Collision Detection

In order to prevent objects occupying different Spaces from passing through, the pick-up and manipulation of tools and parts involved in gearbox virtual maintenance training must reflect the collision phenomenon in real operation in virtual training scenes⁵. Collision problems in maintenance training include collision detection and collision corresponding. Generally, collision detection algorithms between geometric models in virtual environment are divided

into two types: spatial decomposition method and hierarchical bounding box method. The structure of gearbox is complex, with many and irregular parts, so it cannot be used for collision detection by spatial decomposition method, so only the hierarchical bounding box method can be used.

Collision detection and processing between parts model and model, model and virtual scene, model and tool based on hierarchical bounding box method can avoid possible phenomena in operation, and further enhance the sense of immersion and reality of virtual scene. Hierarchical bounding box algorithms are mainly divided into the following categories: axial enclosure (AABB), square bounding box (OBB), bounding Sphere (Sphere), directional polyhedron (K-DOP), etc., as shown in Figure 5.

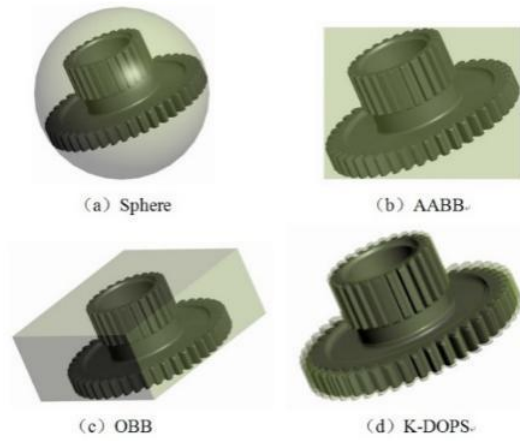


Fig. 5 The classification of the most common bounding boxes

Hereinafter, the advantages and disadvantages of different bounding boxes are analyzed through the time consumption function ⁶.

$$T_{total} = \begin{pmatrix} C_b \\ C_p \\ C_u \\ C_d \end{pmatrix} \bullet \begin{Bmatrix} N_b & N_p & N_u & 1 \end{Bmatrix} \quad (5)$$

T_{total} is the total cost of the intersection test of a pair of geometries; N_b is the bounding box logarithm participating in the intersection test; C_b is the cost of testing the intersection of a pair of bounding boxes; N_p is the logarithm of geometric elements participating in the intersection test; C_p is the cost of testing the intersection of a pair of geometric elements; N_u is the number of bounding boxes that need to be updated after the bounding box object is

translated; C_u to update a translational motion after the bounding box cost; N_v is the number of bounding boxes to be updated after the bounding box is rotated; C_v is the cost of updating a bounding box after rotation; C_d is the cost of updating the bounding box after the object is deformed.

From eq. 4, we can obtain the time consumed in the intersection test of a particular bounding box, the time required to update the bounding box after the object moves and rotates, and the time required to update the bounding box after the object deforms. However, if we want to evaluate the performance of a bounding box in the collision detection process, or seek the basis for selecting an appropriate bounding box, it is still not comprehensive and objective only through calculation of Equation (4). The difficulty of the bounding box construction, the size of the storage space occupied, and the real-time and accuracy requirements of the algorithm are all factors that must be considered. For the convenience of comparison, the optimal value is assumed to be "1", and the performance comparison of various bounding boxes is shown in Table 1:

Table 1 Merits comparison of each bounding box

Enveloping box type	Construction time	Required storage space	Intersection test time	Time required to update the bounding box after the object position changes	Object shape changes after bounding box update cost	Tightness
Square (OBB)	3	3	3	3	4	2
Axial (AABB)	1	2	2	2	1	3
Spherical (Sphere)	2	1	1	1	3	4
Directional polyhedra (K-DOPS)	3	3	3	3	2	1

From Table1, K-DOPS has the best compactness among the four algorithms, and its construction difficulty is between OBB and Sphere. When the logarithm and direction of parallel planes are set properly, the fast and real-time detection can be flexibly balanced with the tightness and accuracy of object surrounding. Combined with the simulation requirements of real time and detection efficiency of the training system, we selected k-DOPS algorithm.

The geometric model of bounding box is a complex polyhedron composed of two parallel planes determined by the fixed direction set, so it is also called fixed direction convex hull ⁷. Its surface is determined by a set of half-space H_i , the outer normal direction of these half

space is selected from the k -th fixed direction (D_1, D_2, \dots, D_k). When design K-DOPS, the elements of the normal vector D_i are always integer coordinate values selected from the group, thus can eliminate the multiplication in calculation and improve computational efficiency. In order to minimize the relevant consumption, the collinear but opposite direction of the vector is usually selected as the normal vector. Accordingly, each K-DOPS actually uses only the amount of directions is $k / 2$, i.e.

$$\begin{aligned}
 D_{i+k/2} &= -D_i \\
 \{x | D_i \cdot x \leq d_i, i=1,2,\dots,k\} &= \bigcap_{i=1}^{k/2} S_i \\
 S_i &= \{x \in R^3 | -d_{i+k/2} \leq D_i \cdot x \leq d_i\}
 \end{aligned} \tag{6}$$

Since the outer normal vector set D of these half-spaces is constant, if D is replaced by a $k \times n$ matrix, Equation (6) can be expressed as:

$$\begin{aligned}
 Dx &\leq b \\
 D &= (d_1, d_2, \dots, d_k), b = (b_{d1}(X), b_{d2}(X), \dots, b_{dk}(X))
 \end{aligned} \tag{7}$$

Since the set of outer normal vectors D of the half-space is constant, $k/2$ normal vectors are predictable, and only $k/2$ values need to be stored in the actual operation. In the intersection test of the same pair of models, only $k/2$ tests are required to construct K-DOPS bounding boxes, which is simpler and less time-consuming than OBB or other forms of bounding boxes for cross-test test.

In the collision detection of object bounding box tree in virtual scene, the traditional traversal detection method is: the bounding box tree $b(S_E)$ of moving object E and the bounding box tree $b(S_F)$ of other objects in the scene, such as F , are detected respectively, and its leaf node V_F is obtained. The leaf node V_F and $b(S_E)$ of F are used for detection, and the leaf node V_E of E is obtained. Finally, V_F and V_E are tested and the test results are obtained. This traversal detection method is clear and easy to design. However, the efficiency is low when dealing with collision detection of objects in complex scenes.

For this reason, a new traversal method is designed in the system, as shown in Figure 6: $b(S_E)$ and $b(S_F)$ are the bounding box trees constructed for object E and F in the scene respectively, and they are simultaneously detected with the surrounding box trees of the other party to obtain their leaf nodes V_E^1, V_E^2, V_F^1 and V_F^2 . Then, V_E^1 was detected at V_F^1 and V_F^2 , and V_E^2 was detected at V_F^1 and V_F^2 , respectively, so as to obtain the detection results of E and F . Compared with traditional methods, this improved traversal detection method can effectively improve the parallelism and efficiency of detection, reduce detection depth, and save storage space.

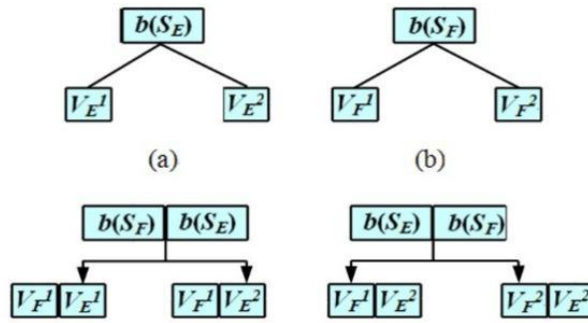
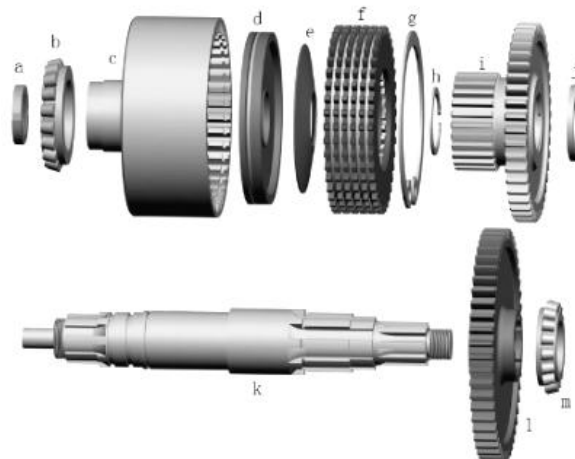


Fig. 6 Optimization of traversal process : (a) bounding box tree constructed for object E; (b) The bounding box tree constructed by object F

In the process of virtual system development, the Collision Manager node in EON software can help to solve the collision problem. Where, the Collision Geometry Type node is mainly used to set the bounding box Type of objects involved in Collision detection. Bounding Spheres, Bounding Sphere, Bounding boxes, Bounding box, Convex Hull, Convex Hulls, Geometry axis and other types are provided for users to choose. The Collision Object node is mainly used to set Collision detection objects and Collision reactions, and the Collision Manager node is used to assist users to manage multiple Collision Object nodes.

3.4 Disassembly sequence planning

The gearbox virtual maintenance training system applies the Petri net theory to the disassembly sequence planning in the transmission virtual disassembly training research, and takes the front gear shaft assembly shown in Figure 7 as an example to establish the disassembly Petri net (DPN) model.



a—lock nut; b—bearing 1; c—clutch hub; d—piston; e—dished spring; f—friction plate; g—check ring 1; h—check ring 2; i—Coupling gear; j—baffle ring; k—Positive shaft; l—single gear; m—bearing 2

Fig. 7 Exploded view of front stop shaft assembly

The method of dismantling the logic network proposed by the model simulation test of the dismantling Petri net is described as: $DPN = (P, T, A, W, C, E, M_0)$

Where: $N = (P, t, a)$ constitutes a directed network diagram

① $P = \{P_1, P_2, \dots, P_N\}$ is the finite set of libraries, ($n > 0$ is the number of libraries), representing parts;

② $T = \{T_1, T_2, \dots, T_M\}$ is a finite set of transitions, ($M > 0$ is the number of transitions), representing disassembly operations;

③ $P \cap T = \Phi \wedge P \cap T > \Phi$;

④ $A \subseteq \{P \times T\} \cup \{T \times P\}$ is the set of directed arcs between libraries and transition

$$A=[a_{ij}] = \begin{cases} -w(i,j) & (\text{when directed arc points from } p_i \text{ to } t_j) \\ w(i,j) & (\text{when directed arc points from } t_j \text{ to } p_i) \\ 0 & (\text{other}) \end{cases} \quad (8)$$

⑤ $W: A \rightarrow \{1, 2, \dots\}$ It is the right of the directed arc between the libraries and the transition, which represents the disassembly operation requirements of the parts;

⑥ C is the inspection and maintenance time of the parts, and E is the disassembly time of the parts;

⑦ $M_0: P \rightarrow \{1, 0, \dots\}$ is the initial identification, which represents the initial state of the components in the DPN model. "1" indicates that the corresponding part has been disassembled; otherwise, "0" indicates that it has not been disassembled;

In this way, the disassembly process planning problem of components is transformed into a Petri net model. All disassembly sequences can be reflected by disassembling Petri nets. The established demolition Petri net model is shown in Figure 8, the library is represented by a circle (○), and the transition is represented by a thick bar (—). The meaning of each variable in the figure is shown in Table 2.

Table 2 variable description of disassembly Petri net

Storehouse	Storage content	transitions	Function description
p1	front stop shaft assembly to be removed	t1	Remove the lock nut
p2~p12	Cluster sub disassembly of parts	t2	Remove the single gear
p13	Remove the obtained lock nut (a)	t3	Remove the bearing 1

p14	Removed bearing 1 (b)	t4	Remove the front stop shaft
p15	Removed clutch hub body (c)	t5	Remove the lock nut
p16	Piston obtained from disassembly (d)	t6	Remove the front stop shaft
p17	Remove the obtained Belleville spring (e)	t7	Remove the front stop shaft
p18	Remove the inner and outer friction plates (f)	t8	Remove the single gear
p19	Remove the obtained retaining ring 1 (g)	t9	Disassemble the clutch hub assembly
p20	Remove the obtained retaining ring 2 (h)	t10	Remove the bearing 1
p21	Removed coupling gear (i)	t11	Remove the front stop shaft
p22	Removed retaining ring (j)	t12	Remove the bearing 1
p23	Remove the front stop shaft (k)	t13	Disassemble the clutch hub assembly
p24	Removed single gear (l)	t14	Remove the coupling gear
p25	Removed bearing 2 (m)	t15	Remove the single gear
		t16	Remove the coupling gear
		t17	Remove the single gear

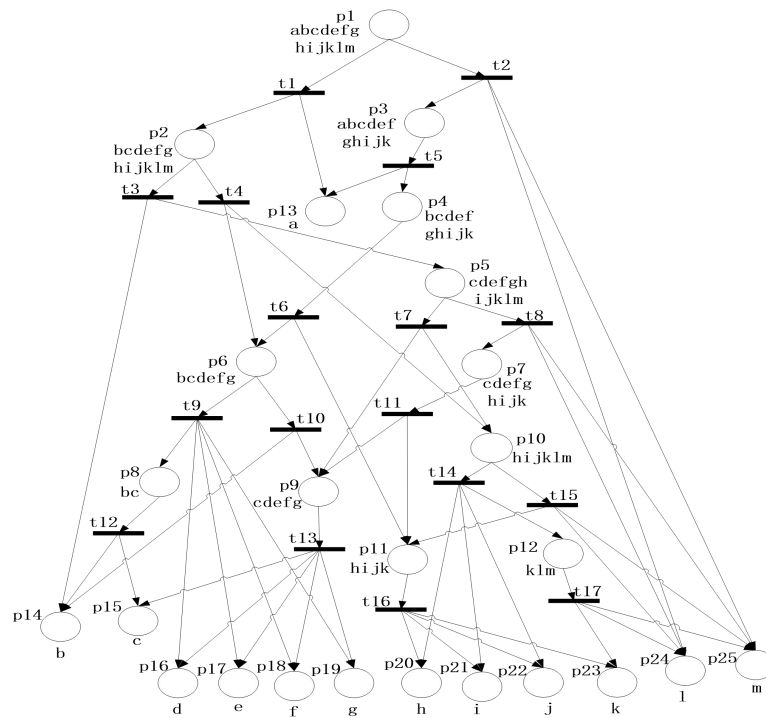


Fig 8 DPN model of front gear shaft assembly

For any dismantling Petri net, let U_k be a $(m \times 1)$ dimensional vector whose i -th element represents the number of times the transition $t_i \in T$ (dismantling operation) occurs in the dismantling process. When $u_i=0$, it means that the corresponding disassembly operation does not occur. Because the transition set T , that is, the dismantling operation is ordered, the vector U_k represents the number and order of the vectors of the number and dimension of transitions,

thereby determining the dismantling sequence.

Let D be the association matrix of the Petri net, and M be the final mark, representing the final state of disassembly.

$$DU_k = M - M_0 \quad (9)$$

In the disassembly for the purpose of component maintenance, the main factors affecting the selection of the optimal disassembly sequence are the maintenance time, that is, the component inspection time C , and the disassembly operation time E . The disassembly efficiency refers to the minimum sum of the disassembly operation time and the inspection and maintenance time of the disassembled parts. Therefore, the most efficient disassembly sequence satisfies:

$$B = \text{Min}(C^T M + E^T U_k) \quad (10)$$

Satisfy the constraints:

$$DU_k = M - M_0 \quad (11)$$

a. Complete disassembly sequence

A complete disassembly is to disassemble and obtain all the parts for inspection or maintenance of the equipment, so its final state is certain. At this time, there is no need to compare the inspection time of all components, only the disassembly time is required, so the optimal disassembly sequence satisfies:

$$B = \text{Min}(E^T U_k) \quad (12)$$

Satisfy the constraints:

$$DU_k = M - M_0 \quad (13)$$

In a complete disassembly, since the final state of the disassembly is known, it is: $M = [0 \ 0 \ 0 \ 0 \ 0 \ 0 \ 0 \ 0 \ 0 \ 0 \ 1 \ 1 \ 1 \ 1 \ 1 \ 1 \ 1 \ 1 \ 1 \ 1 \ 1 \ 1]^T$

Based on experience, the dismantling operation time is: $E = [30 \ 20 \ 34 \ 26 \ 30 \ 20 \ 26 \ 20 \ 40 \ 32 \ 20 \ 30 \ 40 \ 34 \ 20 \ 30 \ 20]^T$

The correlation matrix D is:

$$D_{25 \times 17} = \begin{matrix} & t_1 & t_2 & t_3 & t_4 & t_5 & t_6 & t_7 & t_8 & t_9 & t_{10} & t_{11} & t_{12} & t_{13} & t_{14} & t_{15} & t_{16} & t_{17} \\ \begin{matrix} p_1 \\ p_2 \\ p_3 \\ p_4 \\ p_5 \\ p_6 \\ p_7 \\ p_8 \\ p_9 \\ p_{10} \\ p_{11} \\ p_{12} \\ p_{13} \\ p_{14} \\ p_{15} \\ p_{16} \\ p_{17} \\ p_{18} \\ p_{19} \\ p_{20} \\ p_{21} \\ p_{22} \\ p_{23} \\ p_{24} \\ p_{25} \end{matrix} & \begin{bmatrix} -1 & -1 & 0 & 0 & 0 & 0 & 0 & 0 & 0 & 0 & 0 & 0 & 0 & 0 & 0 & 0 & 0 & 0 \\ 1 & 0 & -1 & -1 & 0 & 0 & 0 & 0 & 0 & 0 & 0 & 0 & 0 & 0 & 0 & 0 & 0 & 0 \\ 0 & 1 & 0 & 0 & -1 & 0 & 0 & 0 & 0 & 0 & 0 & 0 & 0 & 0 & 0 & 0 & 0 & 0 \\ 0 & 0 & 0 & 0 & 1 & -1 & 0 & 0 & 0 & 0 & 0 & 0 & 0 & 0 & 0 & 0 & 0 & 0 \\ 0 & 0 & 1 & 0 & 0 & 0 & -1 & -1 & 0 & 0 & 0 & 0 & 0 & 0 & 0 & 0 & 0 & 0 \\ 0 & 0 & 0 & 1 & 0 & 1 & 0 & 0 & -1 & -1 & 0 & 0 & 0 & 0 & 0 & 0 & 0 & 0 \\ 0 & 0 & 0 & 0 & 0 & 0 & 0 & 1 & 0 & 0 & -1 & 0 & 0 & 0 & 0 & 0 & 0 & 0 \\ 0 & 0 & 0 & 0 & 0 & 0 & 1 & 0 & 0 & 1 & 1 & 0 & -1 & 0 & 0 & 0 & 0 & 0 \\ 0 & 0 & 0 & 1 & 0 & 0 & 1 & 0 & 0 & 0 & 0 & 0 & 0 & -1 & -1 & 0 & 0 & 0 \\ 0 & 0 & 0 & 0 & 0 & 1 & 0 & 0 & 0 & 0 & 1 & 0 & 0 & 0 & 1 & 0 & 0 & -1 \\ 0 & 0 & 0 & 0 & 0 & 0 & 0 & 0 & 0 & 0 & 0 & 0 & 0 & 0 & 1 & 0 & 0 & -1 \\ 1 & 0 & 0 & 0 & 1 & 0 & 0 & 0 & 0 & 0 & 0 & 0 & 0 & 0 & 0 & 0 & 0 & 0 \\ 0 & 0 & 1 & 0 & 0 & 0 & 0 & 0 & 0 & 1 & 0 & 1 & 0 & 0 & 0 & 0 & 0 & 0 \\ 0 & 0 & 0 & 0 & 0 & 0 & 0 & 0 & 0 & 0 & 0 & 1 & 1 & 0 & 0 & 0 & 0 & 0 \\ 0 & 0 & 0 & 0 & 0 & 0 & 0 & 0 & 1 & 0 & 0 & 0 & 1 & 0 & 0 & 0 & 0 & 0 \\ 0 & 0 & 0 & 0 & 0 & 0 & 0 & 0 & 1 & 0 & 0 & 0 & 1 & 0 & 0 & 0 & 0 & 0 \\ 0 & 0 & 0 & 0 & 0 & 0 & 0 & 0 & 0 & 0 & 0 & 0 & 0 & 1 & 0 & 1 & 0 & 0 \\ 0 & 0 & 0 & 0 & 0 & 0 & 0 & 0 & 0 & 0 & 0 & 0 & 0 & 1 & 0 & 1 & 0 & 0 \\ 0 & 0 & 0 & 0 & 0 & 0 & 0 & 0 & 0 & 0 & 0 & 0 & 0 & 0 & 0 & 1 & 1 & 1 \\ 0 & 1 & 0 & 0 & 0 & 0 & 0 & 1 & 0 & 0 & 0 & 0 & 0 & 0 & 1 & 0 & 1 & 1 \\ 0 & 1 & 0 & 0 & 0 & 0 & 0 & 1 & 0 & 0 & 0 & 0 & 0 & 0 & 1 & 0 & 1 & 1 \end{bmatrix} \end{matrix}$$

Solving equation (11), the corresponding optimal disassembly sequence is $t_2 \rightarrow t_5 \rightarrow t_6 \rightarrow t_{16} \rightarrow t_9 \rightarrow t_{12}$, and the shortest disassembly time is 170.

b. Target fault part disassembly sequence

The disassembly of the target part in maintenance is usually the disassembly of the faulty part. When part i is a faulty part, let its C_i be a minimum value such as 0, and other normal parts are 100. E and D are the same as before. Assuming that the part p_{16} is a faulty part, then

$$C = [100 \ 100 \ 100 \ 100 \ 100 \ 100 \ 100 \ 100 \ 100 \ 100 \ 100 \ 100 \ 100 \ 100 \ 100 \ 100 \ 0 \ 100 \ 100 \ 100 \ 100 \ 100 \ 100 \ 100 \ 100 \ 100]^T$$

Substituting the above parameters into formula (9), the minimum disassembly time is 96, and the disassembly path is $t_1 \rightarrow t_4 \rightarrow t_9$. The disassembled parts are $p_8, p_{10}, p_{13}, p_{16}, p_{17}, p_{18}, p_{19}$.

After the disassembly inspection by skilled maintenance workers, the disassembly sequence obtained by the method in this paper takes the shortest time.

3.5 Training Evaluation

In order to ensure the training quality of the trainees, obtain reliable test evaluation results, and improve the authenticity and efficiency of the training of the trainees, a training assessment and evaluation system has been established. The assessment of the virtual maintenance training of gearbox is a complex assessment system with many discrete spatial

points, including many uncertain variable factors⁸. In order to improve the training effect of trainees and obtain accurate evaluation results, fuzzy evaluation method is used.

a. Determination of evaluation element set and evaluation grade set

Fuzzy comprehensive evaluation is based on fuzzy mathematics, and it is an effective multi-factor decision-making method to comprehensively evaluate things affected by multiple factors. Fuzzy comprehensive evaluation is to use fuzzy transformation principle and maximum membership principle to judge things affected by many factors. Denote the evaluation factor as $u_i(i=1,2,\dots,m)$ and the evaluation level as $v_j(j=1,2,\dots,n)$, then the evaluation factor set U and the evaluation level set V can be established;

$$\begin{cases} U = (u_1, u_2, \dots, u_m) \\ V = (v_1, v_2, \dots, v_n) \end{cases} \quad (14)$$

Determine the following evaluation elements set U and evaluation level set V of the transmission virtual maintenance training system according to actual production requirements:

$U = (u_1, u_2, u_3, u_4) = (\text{fault analysis, fault location, use of test tools, key operations})$; $V = (v_1, v_2, v_3, v_4) = (\text{excellent, good, qualified, unqualified})$, the evaluation limit $[0, 100]$ of each assessment index is divided into four intervals $[100,90]$, $[89,75]$, $[74,60]$, $[59,0]$.

b. Establish fuzzy comprehensive evaluation matrix

Make a simple evaluation $f(u_i)$ for each factor U_i in the evaluation element set U of transmission virtual maintenance training, then the membership function f can be regarded as the fuzzy mapping of $U \sim V$. through the mapping, the fuzzy evaluation matrix R of frame electrophoresis quality can be inferred:

$$R = (r_{ij})_{n \times m} = \begin{pmatrix} r_{11} & r_{12} & \dots & r_{1m} \\ r_{21} & r_{22} & \dots & r_{2m} \\ \dots & \dots & \dots & \dots \\ r_{n1} & r_{n2} & \dots & r_{nm} \end{pmatrix} \quad (15)$$

In the formula: r_{ij} represents the membership degree of the factor u_i in the factor set U corresponding to the level v_j in the evaluation set V .

c. Weight distribution of evaluation elements

Considering the influence of multiple factors, there is a fuzzy subset $A = \{a_1, a_2, \dots, a_m\}$

on the evaluation factor set U, and there are: $\sum_{i=1}^m a_i = 1$. In the formula, a_i is the weight coefficient of the evaluation factor u_i , that is, the influence degree of a single evaluation factor in the comprehensive evaluation. The weight distribution of the evaluation elements of the gearbox virtual training is determined by the comprehensive analytic hierarchy process and the expert estimation method. The weight value of each element to be selected is: $A=(0.30,0.25,0.2,0.25)$.

d. Comprehensive evaluation

From this, the fuzzy transformation D of $U \sim V$ can be determined:

$D = A \times R = \{d_1, d_2, \dots, d_m\}$, among them, d_j represents the membership degree of the evaluated object corresponding to the evaluation level v_j .

According to the principle of maximum membership, if: $b_{ij} = \max \{b_j : 1 \leq j \leq m\}$, then the grade v_{ji} is determined to be the evaluation grade corresponding to the final evaluation result.

Assume that the score given by the coach to the four evaluation indicators of the virtual maintenance training of a certain person to be assessed is [90, 92, 83, 78], obtained by establishing an evaluation model $D=[0.37, 0.905, 0.629, 0.56]$, and obtained after normalization $D^*=[0.1502, 0.3673, 0.2552, 0.2272]$. According to the principle of maximum membership, the comprehensive evaluation result was good.

4. Module Package and System Design

After the EON virtual simulation platform is used to design and complete each training simulation module, and then the Delphi programming software is used to integrate each module to build a gearbox virtual maintenance training system platform (shown in Figure 9). The construction of the platform is based on the functional design of the system, and the system framework is constructed in the form of buttons and directory trees. By clicking the corresponding button, the corresponding simulation training module is directly entered, and the procedure for calling the virtual disassembly training module is as follows:

```
procedure TF_main.SpeedButton1Click(Sender: TObject);
```

```
begin
```

```
Control11.Visible:=true;
```

```

ShockwaveFlash1.Visible:=false;

Control11.left:=150;

Control11.top:=200;

cxTreeView2.Left:=289;

cxTreeView2.Top:=500;

cxTreeView1.Visible:=true;

    //cxTreeView1.Items[0].Selected:=false;

    //cxTreeView1.Items[1].Selected:=false;

Image1.Picture.LoadFromFile(getcurrentdir+'\pic1.jpg');

Control11.SimulationFile=getcurrentdir+'\baoyang.eoz';

end;

```



Fig. 9 The main interface of the system

5. Conclusion

This paper researches and designs key technologies such as 3D model construction, 3D observation, collision detection and training evaluation in the virtual maintenance training of heavy-duty vehicle gearboxes, and develops a gearbox virtual maintenance training system combined with the EON virtual simulation platform. The verification shows that the system effectively overcomes the unfavorable factors caused by the number of equipment, maintenance costs, training venues and human resources, greatly reduces the input cost of maintenance training, and provides a modern, economical and practical maintenance support training method for new equipment, with significant economic and social benefits.

References

- [1] W.J. Chu, Z.C. Zhu: 3D Motion Simulation of Engineering Equipment Working Mechanism Based on Reverse Drive Mode , Materials Science and Engineering Vol.746(2012), p. 249-254..
- [2] X.F. Zhu, Z.D. Ma, P. Hu: Nonconforming Is geometric Analysis Based on NURBS with Exact Geometry, Chinese Journal of Solid Mechanics Vol.33 (2012), p. 487-492.
- [3] S.C. Yan, J.Z. Zhou, H.J. Zhu, et al: Summary of Collision Detection Algorithms in Virtual Maintenance Training System, Journal of Machine Building & Automation Vol.41 (2012),p. 98-101.
- [4] W.J. Chu, J.Z. Zhou, Q.Z. Tu, et al: Study on Modeling Technology Based on Polygon Transform, Journal of Advanced Materials Research Vol.655 (2013), p.296-299
- [5] T. Larsson, T. Akenine-Moller: Collision Detection for Continuously Deforming Bodies, Journal of Euro graphics Vol. 2001 (2001), p. 325-333.
- [6] J.Z. Zhu, X.P. Xu: Research and Application of K-DOPS Algorithm in Virtual Maintenance Training System for Diesel Engine, Advanced Materials Research Vol. 805-806 (2013), p.1911-1916.
- [7] S.C. Yan, J.Z. Zhou, H.J. Zhu and S.C. Han: Summary of Collision Detection Algorithms in Virtual Maintenance Training System, Journal of Machine Building & Automation Vol.41(2012), p.98-101.
- [8] W.J. Chu, X.h. Hei, Z.C. Zhu: Research on the Semi-physical Simulation Maintenance Training System of One Engineering Equipment, Advances in Intelligent Systems Research Vol.168(2019),p.34-39.